

Particle emission from chemically enhanced electron-beam-induced etching of Si: An approach for zero-energy secondary-ion mass spectrometry

N. Vanhove,^{1,2} P. Lievens,³ and W. Vandervorst^{1,2}

¹IMEC vzw, Kapeldreef 75, B-3001 Leuven, Belgium

²Instituut voor Kern-en Stralingsfysica, K.U. Leuven, Celestijnenlaan 200 D, B-3001 Leuven, Belgium

³Laboratorium voor Vaste-Stoffysica en Magnetisme, K.U. Leuven, Celestijnenlaan 200 D, B-3001 Leuven, Belgium

(Received 15 October 2008; published 6 January 2009)

The mechanisms of particle emission resulting from electron-beam-induced etching of Si surfaces have been studied. A detailed analysis of the obtained mass spectra and kinetic-energy distributions shows that SiF_x ($x=0-2$) species are predominantly desorbed from the surface when exposed to XeF_2 etching gas and the electron beam. Based on these observations, we demonstrate a unique concept for materials analysis, termed zero-energy secondary-ion mass spectrometry, which can provide very high depth resolution and accurate near-surface profiles.

DOI: [10.1103/PhysRevB.79.035305](https://doi.org/10.1103/PhysRevB.79.035305)

PACS number(s): 82.80.Ms, 52.77.Bn, 79.20.La

The interaction of an energetic ion beam with a solid is one of the most frequently used methods for material removal and material analysis. As such ion-beam sputtering has gained wide acceptance as part of material characterization techniques such as Auger electron spectroscopy, x-ray photoelectron spectroscopy, and secondary ion mass spectrometry (SIMS).¹ However, the collision cascade associated with the slowing down of the impinging ion extends over dimensions (5–10 nm) commensurate with film thickness and features size presently studied in nanotechnology. As such the concurrent ion-beam mixing processes are becoming too important and limit the depth and spatial resolutions. Faced with the present interest in quantitatively studying the composition of complex heterogeneous materials, shallow surface layers, and dopant profiles across interfaces with very high depth resolution (subnanometer) and lateral resolution (nanometer), sputtering based characterization techniques become very limited.² Although the collision cascade can be reduced by lowering the primary beam energy, a minimum energy is imposed by the energy threshold for sputtering as well as by the increased efficiency for primary ion deposition versus the effective (substrate) sputter yield at reduced energies.³ Therefore, limiting this energetic interaction requires a sample erosion technique without the formation of a collision cascade, which, for instance, is the case for photon beams or electron beams.

In this work we will therefore exploit electron-beam-induced etching (EBIE) as it appears to combine high depth resolution with high spatial resolution. The absence of a collision cascade requires an alternative process to stimulate the particle emission which is frequently pursued by combining reactive gas exposure with electron-beam irradiation. Such a combination may lead to a local chemical reaction between adsorbed gas molecules and surface atoms induced by the incident electron beam, and thus a local particle emission through an evaporation process from the (surface) adsorbed layer.⁴ Chemically enhanced erosion has already been reported using ion beams. For instance, Coburn and Winters⁵ studied the spontaneous and ion enhanced etchings of Si and SiO_2 with XeF_2 , and reported that the spontaneous etch rate increases linearly with the partial pressure of XeF_2 , whereas

no spontaneous etching of SiO_2 is observed. At room temperature, the major reaction product is SiF_4 , where above 600 K also SiF_2 is desorbed. In the case of the ion enhanced $\text{XeF}_2/\text{Si}/\text{Ar}^+$ etch system, Sebel⁶ showed that the etch rate is enhanced by a factor of eight (dependent on the ion flux) due to a higher SiF_2 desorption (physical sputtering) and a higher formation rate of SiF_4 (chemical sputtering). Molecular-dynamics simulations and experimental results both show that a reaction layer of 10–20 Å is formed consisting of SiF_x ($x=1-3$) groups when a silicon substrate is exposed to fluorine atoms.^{7,8} The amount of published work is still very limited on EBIE and more fundamental studies are necessary to get more insight in which parameters control the etching process.⁴ In this paper we investigate EBIE of Si and B-doped Si upon exposure to XeF_2 with mass spectrometry, thereby introducing a unique surface analysis technique termed zero-energy SIMS. The detailed analysis of mass spectra and kinetic-energy distributions (KEDs) of the volatile EBIE reaction products as presented here is an important step in understanding the fundamental etch mechanisms.

The experiments were carried out with a SIMS tool (Cameca IMS 5f) based on a magnetic sector mass spectrometer, preceded by an electrostatic energy filter. For the EBIE experiments, an electron beam of 6 keV with a diameter of approximately 150 μm in spot mode and a current density of 0.15 A/cm² was used at near normal incidence. XeF_2 was introduced as etching gas through a gas nozzle which is situated approximately 5 mm above the substrate. The corresponding chamber background pressure during the EBIE experiments was around 10⁻⁷ mbar. Mass spectra (and depth profiles) were recorded in the positive mode (sample potential of +4.5 kV) implying that only positive ions which are desorbed from the surface or are created in the gas phase by electron-impact ionization can be detected. The KEDs were determined by ramping the sample accelerating voltage in steps of 1 V while the energy filter was set to an energy band pass of approximately 1 eV. The zero-kinetic-energy point was determined from the KEDs recorded for Si ions. It was taken as the crossing of the tangent of the decaying slope on the low-energy side of the KED with the energy axis.

The mass distributions of the particles leaving a pure sili-

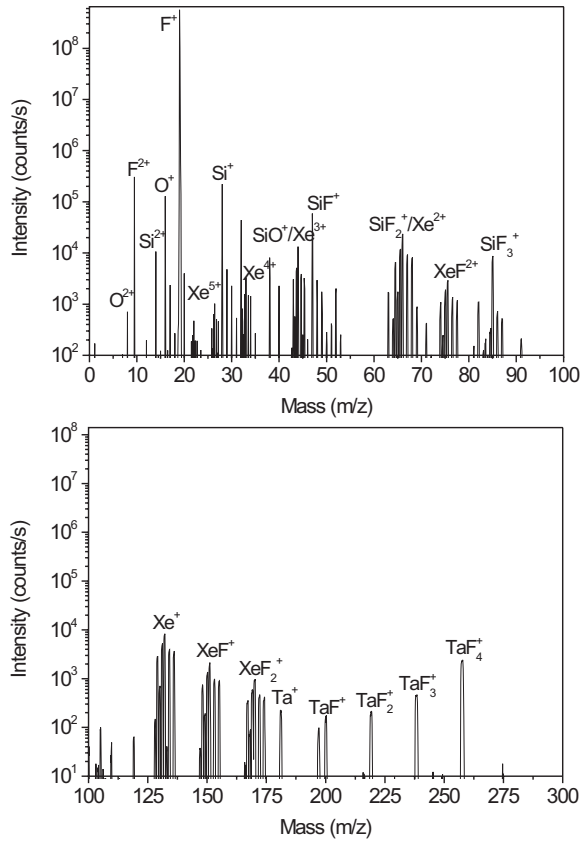


FIG. 1. Mass spectrum of the particles emitted by silicon EBIE with XeF_2 as etching gas in positive mode and steady-state condition.

con substrate in positive mode are shown in Fig. 1. The spectra were taken after prolonged EBIE exposure in the steady-state condition. Both the gas components (Xe, F) and species originating from the sample substrate (Si, SiF, etc.) were observed. Reaction products of the electron-impact ionization of XeF_2 into XeF_2^+ , XeF^+ , and Xe^+ show up, as well as intense Xe^{n+} ($n=1-5$) peaks. The latter result from multiple electron-impact ionization of Xe and their relative intensities are in agreement with the partial ionization cross section of Xe atoms in the gas phase.⁹ The mass peaks at 181, 200, 219, 238, and 257 are most probably TaF_x^+ ($x=0-4$) species, and are due to exposure of the Ta-containing sample holder to the broad electron beam. More important for the Si EBIE process is the observation of the SiF_x^+ ($x=0-3$) species. This demonstrates that different products are formed due to reactions between Si and F atoms, and that erosion of the silicon substrate takes place. SiF_4 gas is also formed by spontaneous XeF_2 etching of silicon at room temperature. Therefore, we compare in Table I the electron-impact ionization and fragmentation pattern of SiF_4 in the gas phase with the observed SiF_x^+ species in the mass spectrum given in Fig. 1. The intensity distribution across the different SiF_x^+ ($x=0-3$) species deviates drastically from the fragmentation pattern resulting from electron-impact dissociation of a SiF_4 gas, indicating that the generated volatile species are not only SiF_4 molecules but also smaller SiF_x molecules. To study the silicon EBIE mechanism in more

TABLE I. Comparison of the observed SiF_x^+ ($x=0-3$) species (see Fig. 1) bombarded with 6 keV electrons and XeF_2 molecules with the most abundant reaction products of dissociative electron-impact ionization of SiF_4 gas with 900 eV electrons (Ref. 10). The intensities are normalized to SiF_3^+ .

Species	Mass	Count rate	SiF_4 (gas)
Si^+	28	26.7	0.102
SiF^+	47	6.6	0.069
SiF_2^+	66	1.22	0.017
SiF_3^+	85	1	1

detail, the KEDs of Xe^+ , F^+ , and the SiF_x^+ ($x=0-3$) species are shown in Fig. 2. Basically one can distinguish three different types of KEDs depending on whether they only show intensities at negative energies without (Xe^+) or with a strong peak around zero (SiF_x^+), and eventually even an additional tail for positive energies (Si^+). In all cases, the intensities observed at negative energies represent an energy deficiency relative to ions originating from the sample surface and are thus characteristic for gas phase ionization. Indeed as the ions are created above the sample surface, they do not experience the full acceleration potential and appear with an energy deficit. Species such as F^+ , Si^+ , and SiF^+ are showing an additional (strong) peak around 0 eV which indicates that these signals are caused by ionized molecules originating from the sample surface. These are the true volatile components emitted during the EBIE process. The absence of these peaks for Xe^+ , SiF_2^+ , and SiF_3^+ indicates that the Xe does not adsorb on the silicon surface, and that the ionized SiF_2 and SiF_3 species are created in the gas phase. In contrast to the mass spectra observed in the case of spontaneous etching (without an electron beam), the contribution of SiF_4 is minimal. This may indicate that SiF_4 is only a minor reaction product in the EBIE process of silicon. The SiF_3^+ signal can be explained by the dissociative ionization of SiF_4

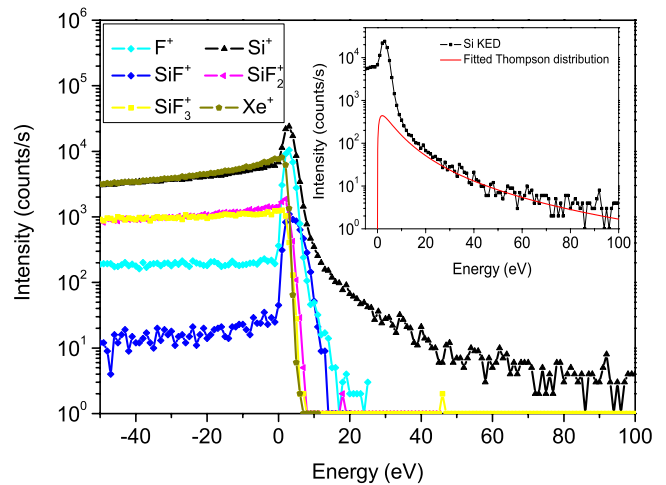


FIG. 2. (Color online) KEDs of Xe^+ , F^+ , and SiF_x^+ ($x=0-3$) species emitted by silicon EBIE with XeF_2 as etching gas in positive mode. The inset shows a fitted Thompson distribution of the high energy tail of the Si KED.

in the gas phase (see Table I). However, the large contribution of SiF_2^+ is in contrast with the dissociative ionization pattern of SiF_4 in the gas phase (see Table I). Note that a straightforward interpretation of the SiF_2^+ signal is hampered by a mass interference with Xe^{2+} . Therefore, the contribution of SiF_2^+ is estimated by subtracting the Xe^{2+} signal which was calculated by the known isotopic abundance of xenon. The strong peak for the Si^+ species around zero energy indicates that the latter is also predominantly emitted as a volatile compound. The small tail extending toward larger positive energies is characteristic for the KED of a sputtered particle and was surprisingly only observed with the Si KED. In the inset of Fig. 2, the tail of the Si KED is fitted with a Thompson energy distribution. The latter could originate from (unintentional) sputter bombardment of the substrate by negative gas phase ions (e.g., F^-) which can be created by an electron attachment process. These anions will be accelerated toward the sample surface by the extraction field. This component can be reduced significantly in an improved setup using lower gas pressures and extraction voltages. From Fig. 2 and Table I, it is clear that the major influence of the electrons is the enhancement of F^+ , Si^+ , and SiF^+ emissions. The KEDs of these species are characterized by a narrow full width at half maximum (FWHM) (≈ 4 eV) approximately Gaussian energy distribution which is typically observed in an electron stimulated desorption (ESD) process. For all the SiF_x^+ ($x=0-2$) species, the exact reaction pathways are difficult to reconstruct since threshold data (i.e., ion intensities as a function of electron energy) at low electron energies could not be obtained because of the high acceleration field at the surface in our setup. In general, the electron beam will (multiple) ionize/excite the adsorbed species and therefore create weakly bound SiF_x species. These excited species can Auger decay and lead to an electron loss from a negatively charged fluorine atom or can create multiple hole states in the case of multiple ionization.^{11,12} Finally, emission of the particles can occur by Coulomb repulsion, which can explain the peak of the KEDs at a few eV for Si^+ , F^+ , and SiF^+ , or emission of neutral (excited) SiF_x species with a decreased surface binding energy can take place. For example, subsequent dissociative ionization of SiF_3 in the gas phase can induce the observation of the SiF_2^+ signal. The presence of a thermal component in all the KEDs is difficult to analyze because the energy resolution of the KEDs is limited to 1 eV. However, due to the low power of the electron beam and the good thermal conductivity of silicon, the influence of a thermal-desorption process should be limited.

It is clear that the EBIE process does not induce any collision cascade and that species emitted as volatile molecules originate from the outermost surface. Thus when combined with a mass spectrometer, as done in the present work, it does represent an ideal depth profiling concept with (theoretically) monolayer resolution approaching the desired performance (depth resolution = 0.5 nm/dec) for semiconductor applications.³ This concept is termed zero-energy SIMS,^{13,14} and an assessment is presented here, a proof of principle of the technique. A depth profile of a highly doped boron chemical vapor deposition (CVD) box is measured with the zero-energy SIMS technique and compared with ultralow-energy SIMS as shown in Fig. 3. The regular SIMS profile

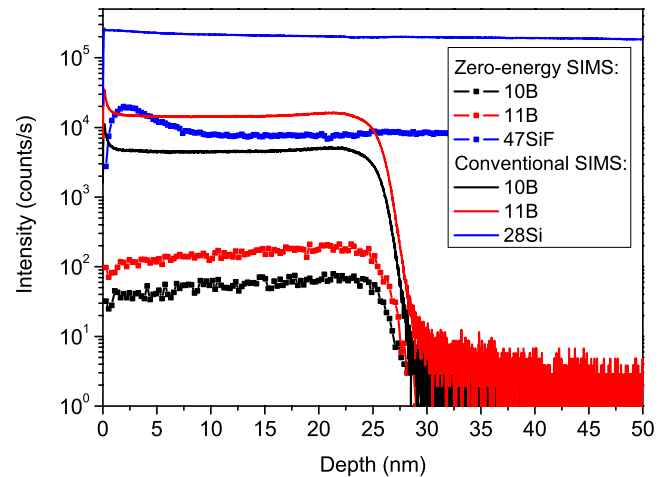


FIG. 3. (Color online) Depth profile of a highly doped boron CVD box analyzed with the zero-energy SIMS technique and compared with conventional SIMS.

was obtained with a Cameca SC Ultra instrument using a 25 nA 150 eV O_2^+ beam and achieves a depth resolution of approximately 1 nm/dec. However the latter can only be achieved with very slow erosion rate (0.1 nm/min with a 25 nA 150 eV oxygen beam, raster size of $400 \times 400 \mu\text{m}^2$) due to the intrinsically low sputter yield and the low current density due to a poorer current generation and transport in the ion source at extremely low energy.

A similar analysis was made with our zero-energy SIMS concept. In this case the electron beam was rastered over an area of $250 \times 250 \mu\text{m}^2$ with XeF_2 as etching gas. As the sample was covered with a native oxide (which shows in principle no etching with XeF_2), no etching should occur. However the cross section of an optical image shown in Fig. 4 clearly indicates that the oxide acted as a mask against spontaneous etching and that only in the electron irradiated area can material removed be observed. We assume that the electron beam leads to a reduction in the native oxide such that etching can be initiated. Once the oxide is removed, etching of the underlying Si is stimulated by the EBIE pro-

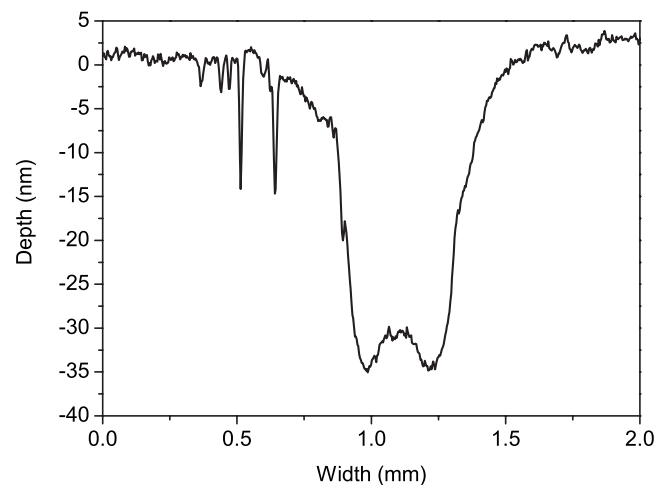


FIG. 4. Cross section of a silicon EBIE crater with XeF_2 as etching gas obtained with an optical profilometer.

cess. Note that, when the native oxide is mechanically damaged (by poor specimen handling), spontaneous etching of silicon can occur through these scratches and pinholes (see Fig. 4). The zero-energy SIMS depth profile shown in Fig. 3 illustrates that at present a depth resolution of 1.5 nm/dec can be achieved. This is a very encouraging result since a non-optimized setup has been used for this assessment. Indeed the depth resolution in depth profiling mode is not only influenced by the nature of the material removal process (layer by layer?) but equally well by its uniformity across the analysis area. Although the electron beam was rastered over the sample, it is clearly visible that the etch rate at the border of the crater is large compared to the center of the crater. Obviously the beam focus of the electron gun was too limited to obtain a completely uniform etching. On the fundamental side, surface roughness can also be created by the penetration of fluorine atoms into the silicon lattice due to steric effects and subsequent concurrent spontaneous etching of the silicon substrate during the EBIE process. The interactions in the XeF_2/Si system create an insulating SiF_x layer up to 10–20 Å followed by a constant concentration of fluorine over at least 200 Å.⁷ These issues could be solved by using other gas (mixtures) instead of XeF_2 as precursor molecules. The properties of chlorine (Cl_2) are very promising for Si EBIE; there is no spontaneous etching of silicon and chlorine saturates the surface to just over 1 monolayer at room temperature.¹⁵

Another interesting aspect of the zero-energy SIMS concept is the absence of any (detectable) surface transients (cf. the flat B profile up to the surface). This is in contrast to the pronounced surface transients and B pileup when SIMS is used, where the buildup of the altered layer and the large desorbing flux of primary ions under full oxidation conditions promotes the migration of boron atoms toward the surface leading to the strong B pileup visible in Fig. 3.¹⁶ Therefore, reliable depth profiles in the first nanometers near the

surface is very difficult to achieve with conventional SIMS. With zero-energy SIMS, no boron peak is observed near the surface region. In this case, the ionization process is only dependent on electron-impact ionization in contrast with conventional SIMS where the ionization process is largely dependent on surface chemistry. Therefore, with zero-energy SIMS it is possible to obtain quantitative information in the surface region together with a high depth resolution on a reasonable time scale. Present erosion velocities are in the order of ≈ 1 nm/min. At present the cations detected originate from the electron-beam-induced ionization process. The latter suffers from a poor efficiency leading to a useful yield for boron of around 10^{-8} in the present implementation. This value can still be increased with several orders of magnitude by the more efficient laser postionization process with femtosecond laser pulses.¹⁷

In this paper, we have analyzed in detail the particle emission resulting from chemically enhanced EBIE. The analysis of the mass spectra and the KEDs shows that the process predominantly leads to the emission of F, Si, and SiF which is very different from the electron-beam-induced decomposition of SiF_4 . When implemented as a tool for material analysis (zero-energy SIMS), the technique becomes very interesting because it eliminates the fundamental limitations concerning ion-beam-induced removal of substrate atoms (mixing and surface transients). Improvements with respect to the implementation will be based on implementing laser postionization to increase the sensitivity of the technique, a fine focused electron beam to form a well defined etch crater, and the use of alternative gases such as chlorine, ultimately aiming at surface analysis with monolayer resolution.

We thank the Belgian Fund for Scientific Research-Flanders (FWO), the Flemish Concerted Action (GOA), and the Federal Interuniversity Attraction Poles (IAP) Research Programs for financial support.

¹F. Adams, L. Van Vaeck, and R. Barrett, *Spectrochim. Acta, Part B* **60**, 13 (2005).

²ITRS, Metrology 2006, <http://www.itrs.net/>.

³W. Vandervorst, *Appl. Surf. Sci.* **255**, 805 (2008).

⁴S. J. Randolph, J. D. Fowlkes, and P. D. Rack, *Crit. Rev. Solid State Mater. Sci.* **31**, 55 (2006).

⁵H. F. Winters and J. W. Coburn, *Appl. Phys. Lett.* **34**, 70 (1979).

⁶P. Sebel, Ph.D. thesis, Eindhoven University of Technology, 1999.

⁷Harold F. Winters, D. B. Graves, D. Humbird, and Sven Tougaard, *J. Vac. Sci. Technol. A* **25**, 96 (2007).

⁸D. Humbird and D. B. Graves, *J. Appl. Phys.* **96**, 791 (2004).

⁹D. P. Almeida, *J. Electron Spectrosc. Relat. Phenom.* **122**, 1 (2002).

¹⁰R. Basner, M. Schmidt, E. Denisov, K. Becker, and H. Deutsch,

J. Chem. Phys. **114**, 1170 (2001).

¹¹M. L. Knotek and P. J. Feibelman, *Phys. Rev. Lett.* **40**, 964 (1978).

¹²C. D. Lane, K. R. Shepperd, A. B. Aleksandrov, and T. M. Orlando, *Surf. Sci.* **593**, 173 (2005).

¹³W. Vandervorst, U.S. Patent No. 20030127591 (10 July 2003).

¹⁴N. Vanhove, P. Lievens, and W. Vandervorst, *Appl. Surf. Sci.* **255**, 1360 (2008).

¹⁵D. Humbird and D. B. Graves, *J. Chem. Phys.* **120**, 2405 (2004).

¹⁶W. Vandervorst, T. Janssens, B. Brijs, T. Conrad, C. Huyghebaert, J. Frühauf, A. Bergmaier, G. Dollinger, T. Buyuklimanli, J. A. VandenBerg, and K. Kimura, *Appl. Surf. Sci.* **231-232**, 618 (2004).

¹⁷Y. Higashi, *Spectrochim. Acta, Part B* **54**, 109 (1999).